

1 **Temporal Inhomogeneities in High-Resolution Gridded Precipitation** 2 **Products for the Southeastern United States**

3 Jeremy E. Diem¹

4 ¹Department of Geosciences, Georgia State University, Atlanta, GA, 30303, USA

5 *Correspondence to:* Jeremy E. Diem (jdiem@gsu.edu)

6 **Abstract.** High-resolution gridded precipitation products are widely used in hydroclimatic analyses, yet their temporal stability
7 has not been comprehensively evaluated. This study assesses temporal inhomogeneities in six datasets—Daymet, gridMET,
8 nClimGrid, PRISM AN (All Networks), PRISM LT (Long Term), and TerraClimate—across the southeastern United States
9 during 1980–2024. Annual precipitation totals derived from monthly and daily products were compared with a regional
10 reference time series constructed from 120 U.S. Cooperative Observer Program (COOP) gauges. Residual-mass curves were
11 used to diagnose departures from temporal homogeneity, and split-sample Mann–Whitney U tests identified statistically
12 significant discontinuities. Trend magnitudes were estimated using the nonparametric Kendall–Theil robust line. Significant
13 discontinuities closely aligned with changes in gauge-network composition and documented data-processing procedures.
14 Wetting shifts in Daymet and PRISM AN coincided with rapid expansion of the Community Collaborative Rain, Hail, and
15 Snow (CoCoRaHS) network and declining COOP coverage. Drying biases in nClimGrid and, to a lesser extent, PRISM LT
16 were associated with increasing reliance on Automated Surface Observing System tipping-bucket gauges, which are known to
17 underestimate rainfall. Abrupt step changes in TerraClimate and gridMET corresponded to modifications in input datasets and
18 reprocessing of precipitation forcing fields. The inhomogeneities produced disparate multi-decadal trends ranging from 19 to
19 48 mm dec⁻¹ compared with a non-significant reference trend of 30 mm dec⁻¹. Two product combinations—Daymet–
20 nClimGrid and Daymet–nClimGrid–PRISM LT—showed no statistically significant discontinuities over 1980–2024 and
21 produced trends within 10% of the reference trend. These combinations provide homogeneous, temporally consistent datasets
22 for multi-decadal precipitation analyses across the Southeast. Despite a significant but modest discontinuity, PRISM LT
23 remains a viable individual product with appropriate homogenization, although continued declines in COOP coverage warrant
24 caution. Overall, the results demonstrate that unrecognized inhomogeneities in gridded precipitation products can substantially
25 bias trend assessments and underscore the need to evaluate and, when necessary, combine datasets to ensure temporal stability
26 in long-term hydroclimatic studies.

27 **1 Introduction**

28 High-quality, multi-decadal precipitation data are essential for research and decision-making. Such records enable rigorous
29 assessment of variability and long-term trends (New et al., 2001) and provide a robust foundation for model calibration and

30 evaluation (Döll et al., 2016; Tango et al., 2025). Reliable long-term observations also underpin integrated and adaptive
31 management of water resources, supporting sustainable planning for agriculture, ecosystems, and regional development (Yang
32 et al., 2021; Ferencz et al., 2024).

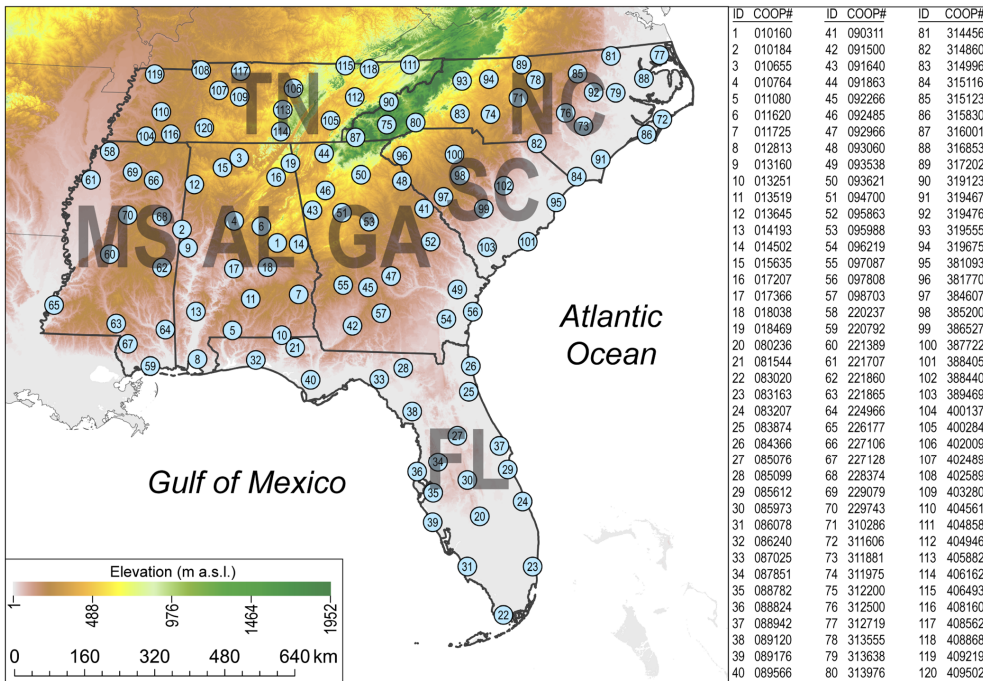
33 Spatial limitations remain a persistent challenge in precipitation measurement. Although gauge networks provide the
34 foundation for precipitation observation, gauge distribution is often sparse and uneven (Kidd et al., 2017). These deficiencies
35 are most pronounced in complex terrain and other data-sparse regions (Michelon et al., 2021).

36 To extend coverage beyond existing gauges, gridded precipitation products were developed. These datasets integrate
37 gauge, satellite, and reanalysis information through interpolation or merging algorithms to generate spatially continuous
38 precipitation estimates (Mankin et al., 2025). Gauge-informed products generally provide higher spatial accuracy than those
39 derived solely from remote sensing or reanalysis (Zandler et al., 2019; Muche et al., 2020; de la Fraga et al., 2024; Mankin et
40 al., 2025). However, the limited availability of gauges in complex terrain still constrains accuracy, and many products perform
41 poorly in mountainous regions (Zandler et al., 2019; de la Fraga et al., 2024; Wang and Tian, 2025).

42 High-resolution gridded precipitation products are particularly well-suited to the needs of the hydrology community,
43 which relies on them more than any other discipline. Gridded precipitation datasets provide the spatially distributed input data
44 required to drive hydrologic models (Livneh et al., 2015; Newman et al., 2015; Shuai et al., 2022). Among many other
45 applications, gridded precipitation products are also employed to quantify basin-scale water balances (Laiti et al., 2018) and
46 to support hydrologic forecasting and management (Mankin et al., 2025).

47 Despite the widespread use of gridded precipitation products, especially within the hydrology community, the temporal
48 stability of these datasets remains insufficiently evaluated. Apparent long-term trends can be distorted by inhomogeneities—
49 systematic, non-climatic shifts in the statistical properties of a time series (Peterson et al., 1998). Only a handful of studies
50 (e.g., Guentchev et al., 2010; Mizukami and Smith, 2012; McAfee et al., 2014; Ferguson and Mocko, 2017; Henn et al., 2018)
51 have explicitly identified or investigated such inhomogeneities in gridded precipitation products. Accordingly, this study
52 evaluates the temporal stability of multiple high-resolution precipitation datasets across a large, climatically uniform region
53 during 1980–2024. The objectives are to (1) detect and characterize temporal inhomogeneities and the factors contributing to
54 them, (2) quantify biases that influence multi-decadal trends, and (3) determine which individual products or product
55 combinations exhibit the greatest temporal stability for regional trend analyses.

56 This study focuses on the southeastern United States (Fig. 1), encompassing Alabama, Florida, Georgia, Mississippi,
57 North Carolina, South Carolina, and Tennessee, with a total area of approximately 882,000 km². The Southeast was selected
58 because much of it has a humid subtropical climate—hot summers, mild winters, and high annual precipitation (Kunkel et al.,
59 2013; Labosier and Quiring, 2013)—and includes numerous long-term reference gauges from the U.S. Cooperative Observer
60 Program (COOP), the nation’s most consistent climate network (National Research Council, 1998).



61
 62 **Figure 1.** Locations of the 120 reference gauges in the southeastern United States. All gauges are part of the U.S. Cooperative Observer
 63 Program (COOP). The seven states that comprise the southeastern United States are Alabama (AL), Florida (FL), Georgia (GA), Mississippi
 64 (MS), North Carolina (NC), South Carolina (SC), and Tennessee (TN).

65 **2 Data**

66 Monthly precipitation totals from a dispersed network of 120 COOP gauges across the Southeast during 1980-2024 were used
 67 to produce a reference time series (Fig. 1). All gauges had at least 90% of months with precipitation totals. Only 1.6% of
 68 gauge-months were missing. The missing monthly totals were replaced with the mean total from the three closest gauges. The
 69 gauges ranged in elevation from 1 m a.s.l. to 668 m a.s.l.; therefore, none of the gauges were located in high-elevation areas.
 70 Monthly totals for each gauge were summed to produce annual precipitation values, which were then averaged across all
 71 gauges to form the regional reference time series. Although COOP provides the longest regional record, documented observer-
 72 related biases indicate that non-climatic variability may persist (Daly et al., 2007).

73 Precipitation estimates were obtained for 1980-2024 from the following high-resolution gridded products: Daymet,
 74 gridMET, nClimGrid, PRISM AN (All Networks), PRISM LT (Long Term), and TerraClimate. Daymet provides daily

75 precipitation estimates for North America at 1-km resolution, with monthly values derived by aggregating daily fields
76 (Thornton et al., 2021). nClimGrid provides daily and monthly precipitation estimates for the conterminous United States at
77 ~4-km resolution, generated independently using climatologically aided interpolation of station data (Vose et al., 2014).
78 PRISM AN provides daily and monthly precipitation estimates for the United States at 30 arc-second (~1 km nominal) spatial
79 resolution, generated using station observations integrated with topographic and other spatial predictors (Daly et al., 2008).
80 Because daily PRISM AN data were not available for 1980, annual totals for that year in the series were derived from monthly
81 PRISM precipitation estimates to maintain a complete 1980–2024 record. PRISM LT data are similar to PRISM AN but are
82 available only at monthly time steps and incorporate substantially fewer gauge networks than the AN product, a design choice
83 intended to improve temporal stability for long-term analyses (Daly et al., 2021). gridMET provides daily precipitation
84 estimates for the conterminous United States at ~4-km resolution, generated by combining high-resolution PRISM
85 climatologies with temporally varying fields from the North American Land Data Assimilation System (NLDAS-2) using the
86 METDATA downscaling method (Abatzoglou, 2013). TerraClimate provides monthly precipitation estimates for the global
87 land surface at ~4-km resolution, generated by combining WorldClim climatologies with time-varying anomalies derived
88 primarily from the Climatic Research Unit Time Series (CRU TS) and Japanese 55-year Reanalysis (JRA-55) datasets
89 (Abatzoglou et al., 2018). When calculating regional means, which were compared with the mean of the 120 COOP gauges,
90 approximately 2.5% of grid cells (those exceeding 668 m a.s.l.) were excluded to restrict the analysis to low- and mid-elevation
91 portions of the Southeast and minimize precipitation inaccuracies associated with mountainous areas.

92 Information on precipitation gauges underlying each gridded product was compiled for 1980–2024. Gauges were
93 classified by network, and spatial coverage was assessed by identifying the 40-km grid cell containing each gauge across the
94 Southeast. For each network, the number of grid cells containing at least one gauge was tallied and divided by the total number
95 of grid cells in the region to calculate percent coverage.

96 In addition to analyzing each gridded product individually, time series were generated for all possible pairwise and multi-
97 product combinations. Combinations were produced separately for the daily and monthly datasets, with each series calculated
98 as the mean of the contributing products (e.g., Daymet and nClimGrid). At each temporal scale, four products were available,
99 yielding six two-product combinations, four three-product combinations, and one four-product combination, for a total of 11
100 unique combinations.

101 **3 Methods**

102 **3.1 Evaluating Spatial Agreement among Precipitation Products**

103 To evaluate spatial agreement and quantify inter-product differences in annual precipitation totals, several complementary
104 comparative analyses were conducted. All six precipitation products were resampled to a common 1-km spatial resolution to
105 ensure direct cell-by-cell comparability across the southeastern United States. Cell-specific percent differences in mean annual
106 precipitation totals over the 1980–2024 period (45-year mean) were calculated for all pairwise combinations of products (15

107 total comparisons). These calculations produced spatially explicit surfaces representing the magnitude and direction of inter-
108 product differences. To quantify the overall level of agreement, the percentage of the 879,861 grid cells exhibiting absolute
109 differences within $\pm 5\%$ was computed for each pairwise comparison.

110 3.2 Residual-Mass Curves

111 Residual-mass curves were constructed as a diagnostic of the homogeneity of precipitation time series and combinations of
112 those series. This approach originates from hydrological consistency testing, in which cumulative residuals are plotted over
113 time to reveal systematic deviations (Searcy and Hardison, 1960). In this study, residuals were obtained from linear regressions
114 in which the reference time series served as the predictor and the product time series as the predictand. For a homogeneous
115 record, the cumulative residuals are expected to remain near zero, fluctuating randomly without systematic drift, whereas
116 sustained deviations or changes in slope indicate shifts, biases, or other inconsistencies (Buishand, 1984; Helsel and Hirsch,
117 2002).

118 3.3 Testing for Differences

119 To identify the most significant discontinuity—defined here as an abrupt, non-climatic shift in a time series representing a
120 temporal inhomogeneity—in each product time series, a nonparametric split-sample approach was applied. For each potential
121 breakpoint year, residuals (i.e., observations minus product estimates) before and after that year were compared using the
122 Mann–Whitney U test ($\alpha = 0.01$, two-tailed), with a minimum of eight years required in each group, yielding candidate
123 breakpoints between 1988 and 2017. The Mann–Whitney U test has been shown to be effective for identifying shifts in
124 hydroclimatic time series (Yue and Wang, 2002), and similar split-sample approaches have been applied in climate
125 homogenization studies to test for differences before and after potential discontinuities (Easterling and Peterson, 1995).

126 3.4 Trend Analyses

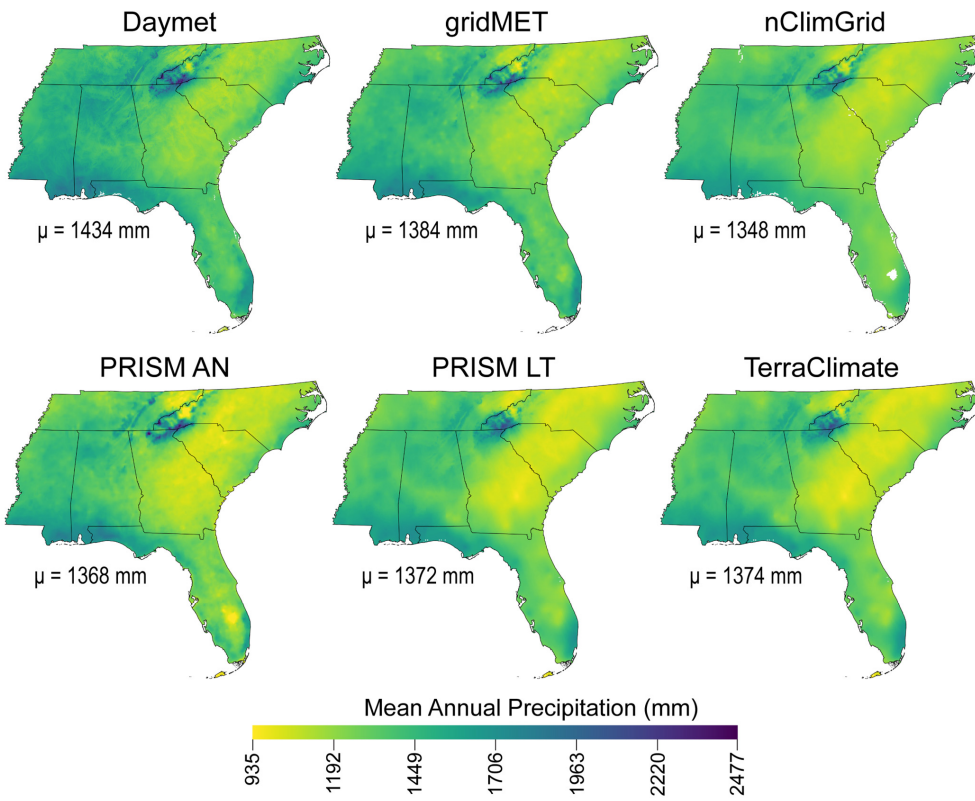
127 Trends in annual precipitation for 1980–2024 were computed for each gridded product and the reference time series. The
128 Kendall–Theil robust line, calculated as the median of the slopes between all pairs of observations (Helsel and Hirsch, 2002),
129 provided a nonparametric estimate of the trend magnitude. The statistical significance of each trend was assessed with
130 Kendall’s tau correlation test ($\alpha = 0.01$, one-tailed).

131 4 Results

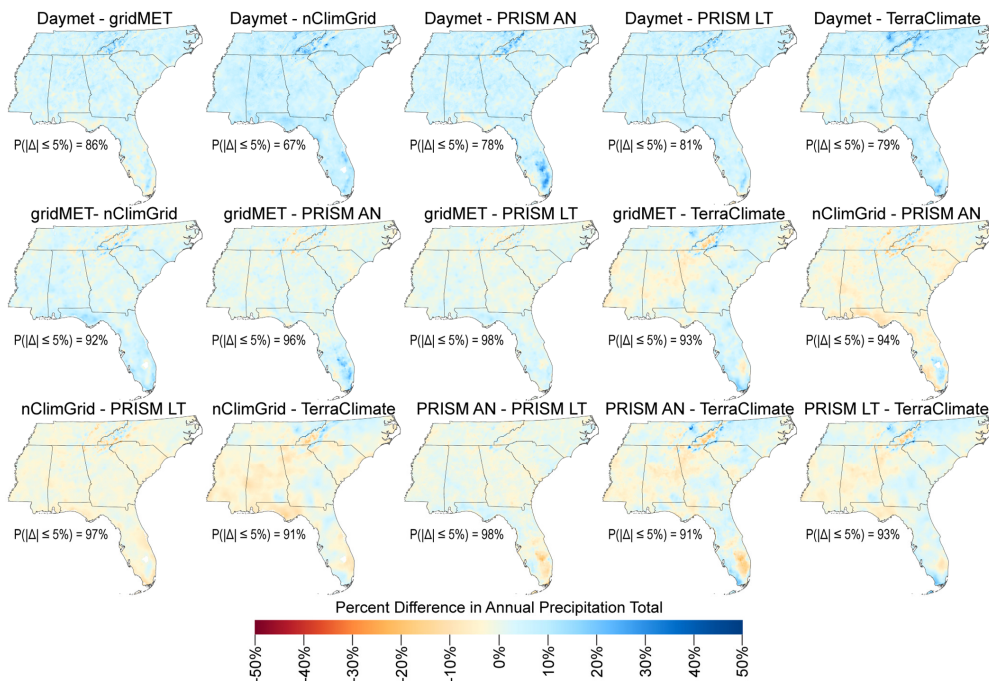
132 4.1 Spatial Agreement among Precipitation Products

133 Mean annual precipitation totals and spatial patterns were broadly consistent among the six precipitation products, with
134 Daymet producing slightly higher totals and nClimGrid slightly lower totals than the others (Figs. 2 and 3). Mean annual totals

135 for 1980–2024 ranged from 1,348 mm for nClimGrid to 1,434 mm for Daymet, with precipitation totals smallest (~1,100 mm)
 136 across central Georgia, South Carolina, and North Carolina and largest (~2,000 mm) in the Blue Ridge and Cumberland
 137 Mountains (Fig. 2). Inter-product differences in mean annual totals were remarkably small: among the 15 pairwise
 138 combinations, 67% to 98% of grid cells differed by no more than $\pm 5\%$, with a mean of 89% of cells meeting this threshold
 139 (Fig. 3). The largest discrepancies were concentrated in the Appalachian and Cumberland Mountains and in southeastern
 140 Florida, although differences exceeding 15% were rare even in these areas. On average, Daymet produced totals 4.7% higher
 141 on average than the other products, whereas nClimGrid produced totals 2.3% lower on average, indicating modest wet and dry
 142 biases relative to the other products.



143
 144 **Figure 2.** Mean annual precipitation totals (in mm) during 1980-2024 for the six precipitation products. gridMET, nClimGrid, PRISM AN,
 145 PRISM LT, and TerraClimate have been resampled to 1-km resolution to match the resolution of Daymet.



146

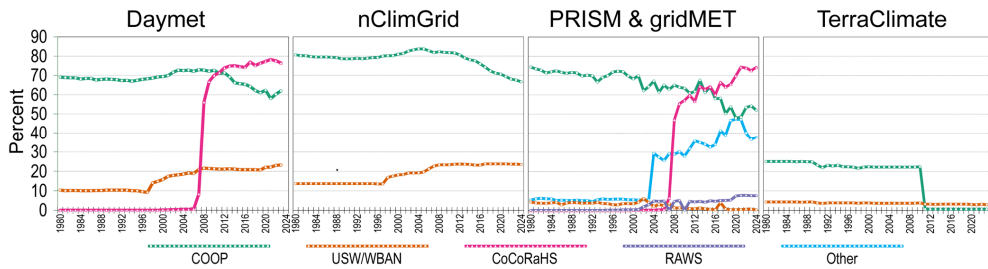
147 **Figure 3.** Percent difference in mean annual precipitation totals (1980–2024) between pairs of products. $P(|\Delta| \leq 5\%)$ is the percentage of grid
 148 cells with percent differences between -5% and 5% .

149

150 4.2 Changes in Gauges

151 All products showed substantial temporal changes in gauge numbers across 1980–2024, most notably increasing coverage by
 152 CoCoRaHS (Community Collaborative Rain, Hail, and Snow Network) gauges and decreasing coverage by COOP gauges
 153 (Fig. 4). Daymet was initially dominated by COOP gauges but by the end of the period CoCoRaHS gauges were most prevalent.
 154 Both CoCoRaHS and first-order airport surface observing stations (hereafter, first-order gauges) increased in coverage, with
 155 CoCoRaHS rising from $<1\%$ in 2006 to 78% in 2021, while COOP gauges began decreasing around 2011. nClimGrid
 156 consistently relied more on COOP than first-order gauges, but the difference in 2024 (67% vs. 24%) was much smaller than
 157 in 1980 (81% vs. 14%). Coverage by first-order gauges began increasing in 1998, while COOP coverage declined after 2012.
 158 PRISM AN and gridMET, which used gauges from 15 networks, showed a similar pattern, with increasing CoCoRaHS and
 159 decreasing COOP coverage. CoCoRaHS coverage rose from $<1\%$ in 2006 to $\sim 75\%$ in 2021. There was also an increase in

160 gauges from other networks and a steady decline in COOP coverage. PRISM LT was dominated by COOP gauges throughout
 161 the period, with COOP comprising between 48% and 74% of all gauges, while first-order gauges accounted for ~4% of
 162 coverage from 1980 to the early 2000s, after which RAWS coverage increased to ~8% by 2024. TerraClimate had much less
 163 gauge coverage overall, with a maximum of 25% from cooperative gauges and an abrupt decline from 22% to <1% between
 164 2010 and 2011.

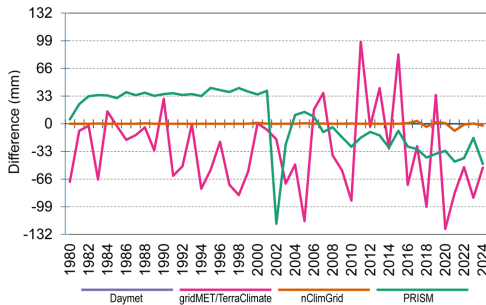


165 **Figure 4.** Percent coverage of the southeastern United States over time by gauge networks used in the precipitation products. COOP is the
 166 U.S. Cooperative Observer Program. USW/WBAN gauges are first-order airport surface observing stations. CoCoRaHS is the Community
 168 Collaborative Rain, Hail and Snow network. RAWS is the Remote Automated Weather Stations network. With respect to the PRISM and
 169 gridMET panel, only COOP, RAWS, and first-order airport (WBAN) gauges are used to develop the PRISM LT product.

170

171 4.3 Comparison of Monthly and Daily Versions of Products

172 Comparisons of monthly and daily product versions revealed consistent behaviour for some datasets but notable temporal
 173 differences for others (Fig. 5). Monthly and daily versions of Daymet and nClimGrid produced either identical or nearly
 174 identical results. In contrast, PRISM AN and PRISM LT exhibited distinct temporal behaviour and are therefore treated
 175 separately in subsequent analyses. Consequently, monthly results—which include TerraClimate and PRISM LT—are shown
 176 in the paper, while the daily results—which include gridMET and PRISM AN—are presented in the supporting information.



177 **Figure 5.** Differences in annual precipitation between totals derived from monthly and versus daily products, 1980–2024. For PRISM, the
 178 monthly product is PRISM LT and the daily product is PRISM AN.
 179

Formatted: Line spacing: Exactly 10 pt

Formatted: Font: Not Bold

180 **4.4 Residual-Mass Curves**

181 Combinations of products produced the most optimal residual-mass curves overall, while performance among individual
182 products varied substantially (Figs. 6 and S1). Optimal curves were characterized by relatively small cumulative sums of the
183 absolute residuals. Among the individual products, PRISM LT exhibited the lowest cumulative residual total, whereas PRISM
184 AN exhibited the highest total. The lowest cumulative sums overall were achieved by several multi-product combinations,
185 including (in ascending order) nClimGrid–PRISM, Daymet–nClimGrid–TerraClimate, Daymet–nClimGrid–PRISM,
186 Daymet–gridMET–nClimGrid, Daymet–nClimGrid, Daymet–nClimGrid–PRISM AN, and Daymet–nClimGrid–PRISM LT.

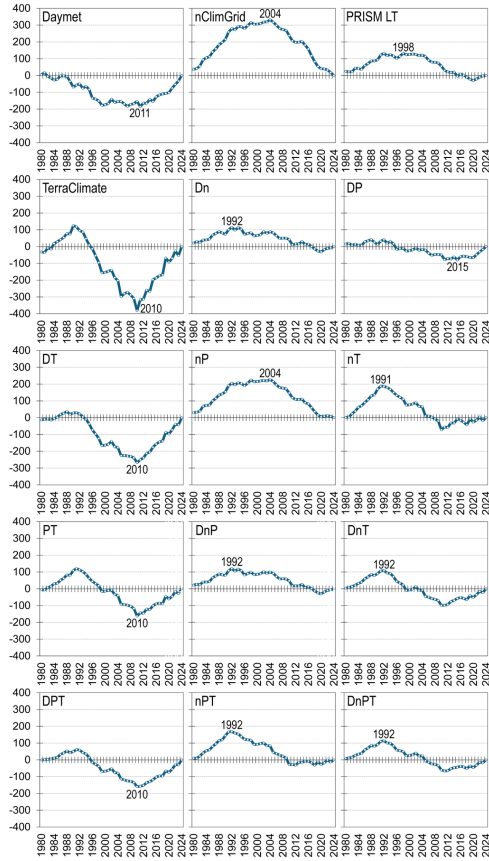
187 The residual-mass curves also revealed potential discontinuities, which occurred between the early 1990s and 2016 (Fig.
188 6 and S1). In each panel of the figures, the year associated with the largest absolute residual corresponded to the year preceding
189 the potential discontinuity. For Daymet, gridMET, nClimGrid, PRISM AN, PRISM LT, and TerraClimate, the potential
190 discontinuities were centered on 2012, 2016, 2005, 2002, 1999, and 2011, respectively. Across all products and product
191 combinations, 50% of the potential discontinuities occurred in 1993 and 2016 combined.

192 **4.5 Discontinuities**

193 Most products exhibited significant discontinuities, and the timing of these shifts generally aligned with the potential
194 discontinuities identified from the residual-mass curves (Figs. 7 and S2). All but three products showed at least one significant
195 discontinuity. The individual products—Daymet, gridMET, nClimGrid, PRISM AN, PRISM LT, and TerraClimate—had
196 discontinuities centered on 2012, 2016, 2005, 2002, 1993, and 2011, respectively. Collectively, discontinuities across all
197 products clustered within five periods: 1991–1993, 2002, 2005, 2011–2012, and 2016. The only products without detectable
198 discontinuities were Daymet–nClimGrid, Daymet–nClimGrid–PRISM LT, and nClimGrid–PRISM AN.

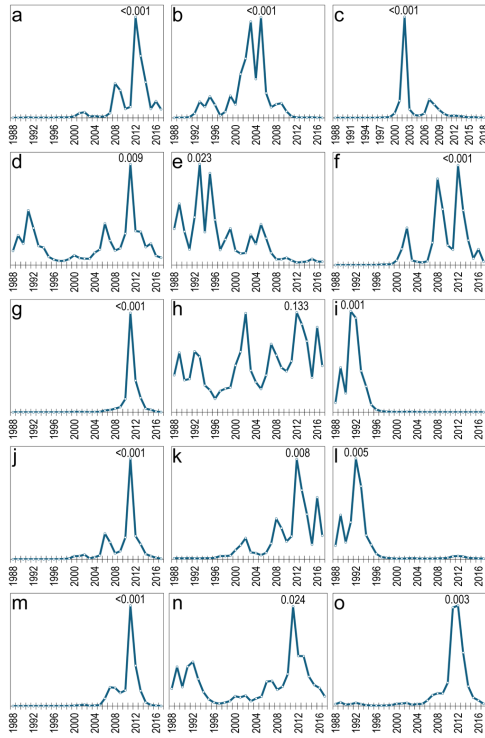
199 **4.6 Time Series of Differences**

200 With respect to differences from the reference time series before and after a discontinuity, most products shifted from either
201 overestimates to larger overestimates, underestimates to larger underestimates, or underestimates to overestimates (Figs. 8 and
202 S3). Daymet shifted from overestimates to larger overestimates. Both gridMET and PRISM AN shifted from underestimates
203 to overestimates. nClimGrid shifted from underestimates to larger underestimates. PRISM LT and TerraClimate were
204 relatively unique among all the products, since PRISM LT shifted from overestimates to underestimates and TerraClimate
205 shifted from underestimates to smaller underestimates.



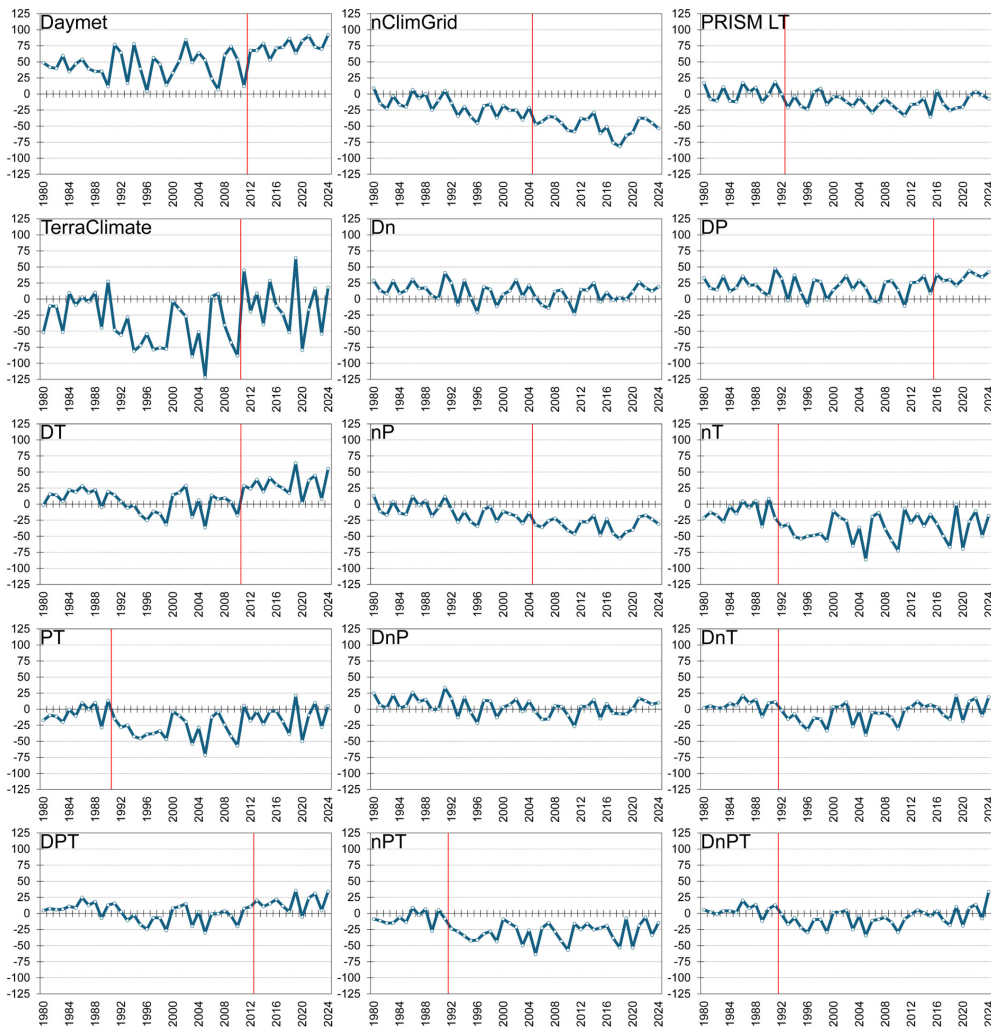
206

207 **Figure 6.** Residual-mass curves for products and combination of products. Abbreviations for Daymet, nClimGrid, PRISM LT, and
 208 TerraClimate, are D, n, P, and T, respectively. Units are mm.



209

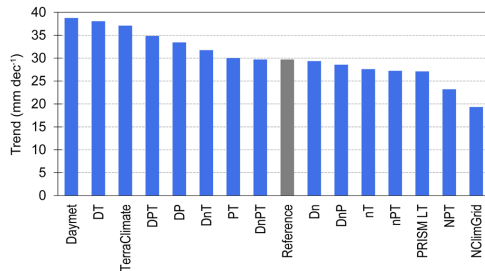
210 **Figure 7.** Inverse p-values for (a) Daymet, (b) nClimGrid, (c) PRISM LT, (d) TerraClimate, (e) Dn, (f) DP, (g) DT, (h) nP, (i) nT, (j) PT,
 211 (k) DnP, (l) DnT, (m) DPT, (n) nPT, and (o) DnPT. Abbreviations for Daymet, nClimGrid, PRISM LT, and TerraClimate, are D, n, P, and
 212 T, respectively. The two-tailed p-values are from Mann-Whitney *U* tests that compared differences from the reference time series before
 213 and after each of the years shown (i.e., 1988-2017).



214
 215 **Figure 8.** Time series of differences (in mm) between the mean of the 120 references gauges and the means for the southeastern United
 216 States that area specific to products and combination of products. Abbreviations for Daymet, nClimGrid, PRISM LT, and TerraClimate,
 217 are D, n, P, and T, respectively.

218 **4.7 Trends**

219 The products exhibited a wide range of precipitation trends, with only a few approximating the reference trend of 30 mm dec⁻¹,
220 which was not statistically significant (Figs. 9 and S4). For the individual products, Daymet, gridMET, nClimGrid, PRISM
221 AN, PRISM LT, and TerraClimate had trends of 39, 39, 19, 48, 27, and 37 mm dec⁻¹, respectively. Among all products, trends
222 ranged from 19 mm dec⁻¹ (nClimGrid) to 48 mm dec⁻¹ (PRISM AN), with PRISM AN being the only product with a
223 statistically significant trend. Products within 10% of the reference trend, listed in ascending order of deviation (with the first
224 product closest to the reference), were Daymet–nClimGrid–PRISM LT–TerraClimate, Daymet–nClimGrid, PRISM LT–
225 TerraClimate, gridMET–nClimGrid, Daymet–nClimGrid–PRISM LT, Daymet–nClimGrid–TerraClimate, nClimGrid–
226 TerraClimate, nClimGrid–PRISM–TerraClimate, and PRISM LT.



227 **Figure 9.** Precipitation increases per decade (in mm) for the reference and 15 other time series. Abbreviations for Daymet, nClimGrid,
228 PRISM LT, and TerraClimate, are D, n, P, and T, respectively.
229

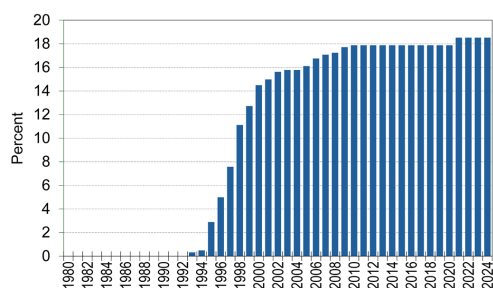
230 **5 Discussion**

231 **5.1 Inhomogeneities and Biased Trends of Products**

232 The proliferation of CoCoRaHS gauges—and to a lesser degree the decline of COOP gauges—caused a wetting bias in the
233 Daymet and PRISM AN time series. Decadal precipitation increases were 28% and 62% larger, respectively, than those from
234 the reference gauges (Figs. 9 and S4). CoCoRaHS gauges generally record slightly higher precipitation totals than COOP
235 gauges, with increases of about 1–5% (Doesken, 2005; CoCoRaHS, 2019; Goble et al., 2019). CoCoRaHS coverage in the
236 Southeast was negligible in 2006 but reached about 75% by 2021, surpassing all other networks by 2012 and 2014 for
237 Daymet and PRISM AN, respectively (Fig. 4). The largest inhomogeneity in the Daymet series occurred in 2012, coinciding
238 with this expansion. Although PRISM AN experienced similar network shifts, its main inhomogeneity appeared in 2002 due
239 to anomalously high precipitation; correcting those values shifts the discontinuity to 2007, aligning with the network
240 transition.

241 The introduction and subsequent expansion of ASOS (Automated Surface Observing Systems) gauges—primarily
242 deployed at airports—along with the decline of COOP gauges, produced a drying bias in nClimGrid and, to a much lesser

243 degree, PRISM LT. The decadal precipitation increases for nClimGrid and PRISM LT were 34% and 9% smaller,
 244 respectively, than that of the reference series (Fig. 9). ASOS instruments use heated tipping-bucket gauges in which each tip
 245 represents 0.01 inch of liquid-equivalent precipitation (Wade, 2003). These gauges underestimate rainfall (Dunn et al.,
 246 2025), with undercatch of 2–10% relative to COOP observations (National Research Council, 2012). ASOS coverage rose
 247 from <1% in 1993 to 19% in 2021 (Fig. 10), while COOP coverage declined from 80% to 70% in nClimGrid and from 67%
 248 to 54% in PRISM LT (Fig. 4). The largest inhomogeneity in nClimGrid occurred in 2005, coinciding with growing ASOS
 249 influence, whereas the largest inhomogeneity in PRISM LT occurred in 1993, coinciding with the introduction of ASOS
 250 gauges.



251
 252 **Figure 10.** Percent coverage of the southeastern United States over time by Automated Surface Observing Systems (ASOS) gauges.

253
 254 Abrupt increases in TerraClimate precipitation totals in 2011 and gridMET totals in 2016 were attributable to changes in
 255 input data. Increases in decadal precipitation for TerraClimate and gridMET were 23% and 28% larger than those of the
 256 reference gauges (Figs. 6 and S5). The TerraClimate shift likely reflected increased influence of JRA-55 anomalies
 257 following a sharp decline in gauge observations (Abatzoglou et al., 2018), while the gridMET inhomogeneity coincided
 258 with a reprocessed precipitation forcing that incorporated late-reporting gauges (Xia et al., 2016).

259 **5.2 Optimal Datasets for Multi-Decadal Precipitation Analyses**

260 Multiple products are suitable for multi-decadal analyses of annual precipitation totals for the southeastern United States. An
 261 optimal product should have three characteristics: (1) a relatively small cumulative residual total in the residual-mass analysis;
 262 (2) no statistically significant discontinuities; and (3) a precipitation trend within 10% of the reference trend. Two product
 263 combinations—Daymet–nClimGrid and Daymet–nClimGrid–PRISM LT—meet these criteria. In these combinations, the
 264 wetting bias in Daymet is offset by the drying biases in nClimGrid and, to a lesser extent, PRISM LT. The result is a temporally
 265 stable series that exhibits no detectable discontinuities and produces a trend closely aligned with the reference time series. A
 266 limitation of these combined datasets is the reduction in spatial resolution resulting from use of nClimGrid, which has ~4-km

267 grid cells that are at least 16 times larger than the ~1-km grids of Daymet and PRISM LT. For applications requiring finer
268 spatial detail, this loss of resolution may be undesirable.

269 PRISM LT also merits consideration as a viable individual product for multi-decadal precipitation analyses. Although the
270 product has a statistically significant discontinuity in 1993, it produced the smallest cumulative residual total among the
271 individual products, and its decadal trend (27 mm dec⁻¹) is within 10% of the reference trend. The 1993–2024 period can be
272 homogenized by applying a multiplicative adjustment factor of 1.0095 derived using the mean-ratio approach outlined by
273 Peterson et al. (1998). However, a potential long-term limitation of PRISM LT is the continued decline in COOP gauge
274 coverage, as the product is dominated by COOP observations and further reductions in that network could decrease spatial
275 representativeness and potentially reduce accuracy over time.

276 **6 Conclusion**

277 Gridded precipitation datasets commonly used for hydroclimatic analyses exhibit substantial temporal inhomogeneities that
278 can distort long-term trend assessments. Evaluation of six high-resolution products and their combinations for the southeastern
279 United States during 1980–2024 revealed statistically significant discontinuities in most series, with shifts clustering in 1991–
280 1993, 2002, 2005, 2011–2012, and 2016 and largely coinciding with changes in gauge networks or data processing. Wetting
281 biases in Daymet and PRISM AN reflected the expansion of CoCoRaHS and decline of COOP gauges, whereas a drying bias
282 in nClimGrid and, to a lesser degree, PRISM LT were associated with increasing influence of ASOS tipping-bucket gauges.
283 Abrupt step changes in TerraClimate and gridMET corresponded to documented shifts in input data and processing. These
284 inhomogeneities produced precipitation trends ranging from 19 to 48 mm dec⁻¹, compared with a non-significant reference
285 trend of 30 mm dec⁻¹. Two product combinations—Daymet–nClimGrid and Daymet–nClimGrid–PRISM LT—removed
286 detectable discontinuities and produced trends within 10% of the reference, indicating improved temporal stability through
287 offsetting wetting and drying biases. Despite a modest discontinuity, PRISM LT also represented a defensible standalone
288 option because of its comparatively small cumulative residuals and near-reference trend. These findings pertain to temporal
289 consistency rather than overall accuracy. Thus, datasets identified as temporally stable may not be optimal for applications
290 requiring accurate day-to-day or location-specific estimates. Overall, the findings underscore the necessity of explicitly
291 evaluating temporal consistency before applying gridded precipitation products in long-term hydroclimatic analyses.

292 *Data availability.* Data used in this paper are available at <https://data.mendeley.com/datasets/37bm8hvpkm/2>.

293 *Competing interests.* The author does not have any competing interests.

294 **References**

- 295 Abatzoglou, J. T.: Development of gridded surface meteorological data for ecological applications and modelling, *Int. J.*
296 *Climatol.*, 33, 121–131, <https://doi.org/10.1002/joc.3413>, 2013.
- 297 Abatzoglou, J. T., Dobrowski, S. Z., Parks, S. A., and Hegewisch, K. C.: TerraClimate, a high-resolution global dataset of
298 monthly climate and climatic water balance from 1958–2015, *Sci. Data*, 5, 170191,
299 <https://doi.org/10.1038/sdata.2017.191>, 2018.
- 300 Buishand, T. A.: Tests for detecting a shift in the mean of hydrological time series, *J. Hydrol.*, 73, 51–69,
301 [https://doi.org/10.1016/0022-1694\(84\)90032-5](https://doi.org/10.1016/0022-1694(84)90032-5), 1984.
- 302 CoCoRaHS (Community Collaborative Rain, Hail & Snow Network): Why CoCoRaHS requires manual measurements,
303 CoCoRaHS Headquarters, Fort Collins, CO, available at:
304 <https://media.cocorahs.org/docs/Why%20CoCoRaHS%20requires%20manual%20measurements.pdf>, 2019.
- 305 Daly, C., Gibson, W. P., Taylor, G. H., Doggett, M. K., and Smith, J. I.: Observer bias in daily precipitation measurements at
306 United States Cooperative Network stations, *Bull. Amer. Meteor. Soc.*, 88, 899–912, [https://doi.org/10.1175/BAMS-88-](https://doi.org/10.1175/BAMS-88-6-899)
307 [6-899](https://doi.org/10.1175/BAMS-88-6-899), 2007.
- 308 Daly, C., Doggett, M. K., Smith, J. I., Olson, K. V., Halbleib, M. D., Dimcovic, Z., Keon, D., Loiselle, R. A., Steinberg, B.,
309 Ryan, A. D., Pancake, C. M., and Kaspar, E. M.: Challenges in observation-based mapping of daily precipitation across
310 the conterminous United States, *J. Atmos. Ocean. Technol.*, 38, 1979–1992, [https://doi.org/10.1175/JTECH-D-21-](https://doi.org/10.1175/JTECH-D-21-0054.1)
311 [0054.1](https://doi.org/10.1175/JTECH-D-21-0054.1), 2021.
- 312 De La Fraga, P., Del-Toro-Guerrero, F. J., Vivoni, E. R., Cavazos, T., and Kretschmar, T.: Evaluation of gridded
313 precipitation datasets in mountainous terrains of Northwestern Mexico, *J. Hydrol.: Reg. Stud.*, 56, 102019,
314 <https://doi.org/10.1016/j.ejrh.2024.102019>, 2024.
- 315 Doesken, N.: A ten-year comparison of daily precipitation from the 4" diameter clear plastic rain gauge versus the 8"
316 diameter metal standard rain gauge, Preprints, 13th Symposium on Meteorological Observations and Instrumentation,
317 Savannah, GA, Amer. Meteor. Soc., available at:
318 https://media.cocorahs.org/docs/AMS_NJD_GaugeComparison_AppldClimate_2-2.pdf.
- 319 Döll, P., Douville, H., Güntner, A., Müller Schmied, H., and Wada, Y.: Modelling freshwater resources at the global scale:
320 challenges and prospects, *Surv. Geophys.*, 37, 195–221, <https://doi.org/10.1007/s10712-015-9343-1>, 2016.
- 321 Durre, I., Arguez, A., Schreck, C. J., Squires, M. F., and Vose, R. S.: Daily high-resolution temperature and precipitation
322 fields for the contiguous United States from 1951 to present, *J. Atmos. Ocean. Technol.*, 39, 1837–1855,
323 <https://doi.org/10.1175/JTECH-D-22-0024.1>, 2022.
- 324 Easterling, D. R. and Peterson, T. C.: A new method for detecting undocumented discontinuities in climatological time
325 series, *Int. J. Climatol.*, 15, 369–377, <https://doi.org/10.1002/joc.3370150403>, 1995.
- 326 Ferencz, S. B., Sun, N., Turner, S. W. D., Smith, B. A., and Rice, J. S.: Multisectoral analysis of drought impacts and
327 management responses to the 2008–2015 record drought in the Colorado Basin, Texas, *Nat. Hazards Earth Syst. Sci.*, 24,
328 1871–1896, <https://doi.org/10.5194/nhess-24-1871-2024>, 2024.
- 329 Ferguson, C. R. and Mocko, D. M.: Diagnosing an artificial trend in NLDAS-2 afternoon precipitation, *J. Hydrometeorol.*,
330 18, 1051–1070, <https://doi.org/10.1175/JHM-D-16-0251.1>, 2017.
- 331 Goble, P. E., Doesken, N. J., Durre, I., Schumacher, R. S., Stewart, A., and Turner, J.: Who received the most rain today?:
332 An analysis of daily precipitation extremes in the contiguous United States using CoCoRaHS and COOP reports, *Bull.*
333 *Am. Meteorol. Soc.*, 101, E710–E719, <https://doi.org/10.1175/BAMS-D-18-0310.1>, 2019.
- 334 Guentchev, G., Barsugli, J. J., and Eischeid, J.: Homogeneity of gridded precipitation datasets for the Colorado River Basin,
335 *J. Appl. Meteorol. Climatol.*, 49, 2404–2415, <https://doi.org/10.1175/2010JAMC2484.1>, 2010.
- 336 Helsel, D. R., and Hirsch, R. M.: Statistical methods in water resources, *Techniques of Water-Resources Investigations*,
337 Book 4, Chapter A3, U.S. Geological Survey, available at: <https://pubs.usgs.gov/twri/twri4a3/>, 2002.
- 338 Henn, B., Newman, A. J., Livneh, B., Daly, C., and Lundquist, J. D.: An assessment of differences in gridded precipitation
339 datasets in complex terrain, *J. Hydrol.*, 556, 1205–1219, <https://doi.org/10.1016/j.jhydrol.2017.03.008>, 2018.
- 340 Kidd, C., Becker, A., Huffman, G. J., Muller, C. L., Joe, P., Skofronick-Jackson, G., and Kirschbaum, D. B.: So, How much
341 of the Earth's surface is covered by rain gauges?, *Bull. Am. Meteorol. Soc.*, 98, 69–78, [https://doi.org/10.1175/BAMS-D-](https://doi.org/10.1175/BAMS-D-14-00283.1)
342 [14-00283.1](https://doi.org/10.1175/BAMS-D-14-00283.1), 2017.

343 Kunkel, K. E., Stevens, L. E., Stevens, S. E., Sun, L., Janssen, E., Wuebbles, D., Konrad, C. E. II, Fuhrman, C. M., Keim, B.
344 D., Kruk, M. C., Billot, A., Needham, H., Shafer, M., and Dobson, J. G.: Regional climate trends and scenarios for the
345 U.S. National Climate Assessment. Part 2: Climate of the Southeast U.S., NOAA Tech. Rep. NESDIS 142-2, National
346 Oceanic and Atmospheric Administration, Washington, DC, 2013.

347 Labosier, C. and Quiring, S.: Hydroclimatology of the Southeastern USA, *Clim. Res.*, 57, 157–171,
348 <https://doi.org/10.3354/cr01166>, 2013.

349 Laiti, L., Mallucci, S., Piccolroaz, S., Bellin, A., Zardi, D., Fiori, A., Nikulin, G., and Majone, B.: Testing the hydrological
350 coherence of high-resolution gridded precipitation and temperature data sets, *Water Resour. Res.*, 54, 1999–2016,
351 <https://doi.org/10.1002/2017WR021633>, 2018.

352 Livneh, B., Bohn, T. J., Pierce, D. W., Munoz-Arriola, F., Nijssen, B., Vose, R., Cayan, D. R., and Brekke, L.: A spatially
353 comprehensive, hydrometeorological data set for Mexico, the U.S., and Southern Canada 1950–2013, *Sci. Data*, 2,
354 150042, <https://doi.org/10.1038/sdata.2015.42>, 2015.

355 Mankin, K. R., Mehan, S., Green, T. R., and Barnard, D. M.: Review of gridded climate products and their use in
356 hydrological analyses reveals overlaps, gaps, and the need for a more objective approach to selecting model forcing
357 datasets, *Hydrol. Earth Syst. Sci.*, 29, 85–108, <https://doi.org/10.5194/hess-29-85-2025>, 2025.

358 McAfee, S., Guentchev, G., and Eischeid, J.: Reconciling precipitation trends in Alaska: 2. Gridded data analyses, *J.*
359 *Geophys. Res.: Atmos.*, 119, <https://doi.org/10.1002/2014JD022461>, 2014.

360 Michelon, A., Benoit, L., Beria, H., Ceperley, N., and Schaeffli, B.: Benefits from high-density rain gauge observations for
361 hydrological response analysis in a small alpine catchment, *Hydrol. Earth Syst. Sci.*, 25, 2301–2325,
362 <https://doi.org/10.5194/hess-25-2301-2021>, 2021.

363 Mizukami, N. and Smith, M. B.: Analysis of inconsistencies in multi-year gridded quantitative precipitation estimate over
364 complex terrain and its impact on hydrologic modeling, *J. Hydrol.*, 428–429, 129–141,
365 <https://doi.org/10.1016/j.jhydrol.2012.01.030>, 2012.

366 Muiche, M. E., Sinnathamby, S., Parmar, R., Knights, C. D., Johnston, J. M., Wolfe, K., Purucker, S. T., Cyterski, M. J., and
367 Smith, D.: Comparison and evaluation of gridded precipitation datasets in a Kansas agricultural watershed using SWAT,
368 *J. Am. Water Resour. Assoc.*, 56, 486–506, <https://doi.org/10.1111/1752-1688.12819>, 2020.

369 National Research Council: Future of the National Weather Service Cooperative Observer Network, The National
370 Academies Press, Washington, DC, 1998.

371 National Research Council: The National Weather Service modernization and associated restructuring: A retrospective
372 assessment, The National Academies Press, Washington, DC, 2012.

373 New, M., Todd, M., Hulme, M., and Jones, P.: Precipitation measurements and trends in the twentieth century, *Intl Journal*
374 *of Climatology*, 21, 1889–1922, <https://doi.org/10.1002/joc.680>, 2001.

375 Newman, A. J., Clark, M. P., Sampson, K., Wood, A., Hay, L. E., Bock, A., Viger, R. J., Blodgett, D., Brekke, L., Arnold, J.
376 R., Hopson, T., and Duan, Q.: Development of a large-sample watershed-scale hydrometeorological data set for the
377 contiguous USA: data set characteristics and assessment of regional variability in hydrologic model performance, *Hydrol.*
378 *Earth Syst. Sci.*, 19, 209–223, <https://doi.org/10.5194/hess-19-209-2015>, 2015.

379 Peterson, T. C., Easterling, D. R., Karl, T. R., Groisman, P., Nicholls, N., Plummer, N., Torok, S., Auer, I., Boehm, R.,
380 Gullett, D., Vincent, L., Heino, R., Tuomenvirta, H., Mestre, O., Szentimrey, T., Salinger, J., Førland, E. J., Hanssen-
381 Bauer, I., Alexandersson, H., Jones, P., and Parker, D.: Homogeneity adjustments of in situ atmospheric climate data: a
382 review, *Int. J. Climatol.*, 18, 1493–1517, [https://doi.org/10.1002/\(SICI\)1097-0088\(19981115\)18:13<1493::AID-
383 JOC329>3.0.CO;2-T](https://doi.org/10.1002/(SICI)1097-0088(19981115)18:13<1493::AID-), 1998.

384 Searcy, J. K., and Hardison, C. H.: Double-mass curves, in: *Manual of Hydrology: Part 1, General Surface-Water*
385 *Techniques*, U.S. Geological Survey Water-Supply Paper 1541-B, 31–66, 1960.

386 Shuai, P., Chen, X., Mital, U., Coon, E. T., and Dwivedi, D.: The effects of spatial and temporal resolution of gridded
387 meteorological forcing on watershed hydrological responses, *Hydrol. Earth Syst. Sci.*, 26, 2245–2276,
388 <https://doi.org/10.5194/hess-26-2245-2022>, 2022.

389 Tang, G., Behrangi, A., Long, D., Li, C., and Hong, Y.: Accounting for spatiotemporal errors of gauges: a critical step to
390 evaluate gridded precipitation products, *J. Hydrol.*, 559, 294–306, <https://doi.org/10.1016/j.jhydrol.2018.02.057>, 2018.

391 Tang, G., Clark, M. P., Knoben, W. J. M., Liu, H., Gharari, S., Arnal, L., Wood, A. W., Newman, A. J., Freer, J., and
392 Papalexiou, S. M.: Uncertainty hotspots in global hydrologic modeling: the impact of precipitation and temperature
393 forcings, *Bull. Am. Meteorol. Soc.*, 106, E146–E166, <https://doi.org/10.1175/BAMS-D-24-0007.1>, 2025.

394 Thornton, P. E., Shrestha, R., Thornton, M., Kao, S.-C., Wei, Y., and Wilson, B. E.: Gridded daily weather data for North
395 America with comprehensive uncertainty quantification, *Sci. Data*, 8, 190, <https://doi.org/10.1038/s41597-021-00973-0>,
396 2021.

397 Vose, R. S., Applequist, S., Squires, M., Durre, I., Menne, M. J., Williams, C. N., Fenimore, C., Gleason, K., and Arndt, D.:
398 Improved historical temperature and precipitation time series for U.S. climate divisions, *J. Appl. Meteorol. Climatol.*, 53,
399 1232–1251, <https://doi.org/10.1175/JAMC-D-13-0248.1>, 2014.

400 Wade, C. G.: A multisensor approach to detecting drizzle on ASOS*, *J. Atmos. Oceanic Technol.*, 20, 820–832,
401 [https://doi.org/10.1175/1520-0426\(2003\)020<0820:AMATDD>2.0.CO;2](https://doi.org/10.1175/1520-0426(2003)020<0820:AMATDD>2.0.CO;2), 2003.

402 Wang, F. and Tian, D.: Hourly Evaluation of eight gridded precipitation datasets over the contiguous United States:
403 intercomparison of satellite, radar, reanalysis, and merged products, *J. Hydrometeorol.*, 26, 1717–1733,
404 <https://doi.org/10.1175/JHM-D-25-0063.1>, 2025.

405 Xia, Y., Mocko, D., and Rodell, M.: An upgrade from current OPS NLDAS-2 system, in: Conference Presentation, NASA
406 Goddard Space Flight Center, 7 July 2016.

407 Yang, D., Yang, Y., and Xia, J.: Hydrological cycle and water resources in a changing world: a review, *Geogr. Sustain.*, 2,
408 115–122, <https://doi.org/10.1016/j.geosus.2021.05.003>, 2021.

409 Yue, S. and Wang, C. Y.: Power of the Mann-Whitney test for detecting a shift in median or mean of hydro-meteorological
410 data, *Stoch. Environ. Res. Risk Assess.*, 16, 307–323, <https://doi.org/10.1007/s00477-002-0101-9>, 2002.

411 Zandler, H., Haag, I., and Samimi, C.: Evaluation needs and temporal performance differences of gridded precipitation
412 products in peripheral mountain regions, *Sci. Rep.*, 9, 15118, <https://doi.org/10.1038/s41598-019-51666-z>, 2019.